Heliyon 10 (2024) e23506

Contents lists available at ScienceDirect

Heliyon

journal homepage: www.cell.com/heliyon

CSTB accelerates the progression of hepatocellular carcinoma via the ERK/AKT/mTOR signaling pathway

Weiyi Zhu [a], Xiangjun Dong [a], Na Tian [a], Zijuan Feng [a], Weihui Zhou [a,*], Weihong Song [a,b,c,**]

[a] *Chongqing Key Laboratory of Translational Medical Research in Cognitive Development and Learning and Memory Disorders, Ministry of Education Key Laboratory of Child Development and Disorders, National Clinical Research Center for Child Health and Disorders, China International Science and Technology Cooperation Base of Child Development and Critical Disorders, Children's Hospital of Chongqing Medical University, Chongqing, China*

[b] *Institute of Aging, Key Laboratory of Alzheimer's Disease of Zhejiang Province, Zhejiang Provincial Clinical Research Center for Mental Disorders, School of Mental Health and Kangning Hospital, The Second Affiliated Hospital and Yuying Children's Hospital, Wenzhou Medical University, Wenzhou, Zhejiang 325000, China*

[c] *Oujiang Laboratory (Zhejiang Lab for Regenerative Medicine, Vision and Brain Health), Wenzhou, Zhejiang 325001, China*

ARTICLE INFO

Keywords:
CSTB
HCC
Proliferation
Cell cycle arrest
EMT
ERK/AKT/mTOR signaling pathway

ABSTRACT

Hepatocellular carcinoma (HCC) is a significant contributor to global cancer-related deaths, leading to high mortality rates. However, the pathogenesis of HCC remains unclear. In this research, by the bioinformatics data analysis, we found that elevated *CSTB* expression correlated with advanced disease and predicted diminished overall survival (OS) in HCC patients. We subsequently verified the oncogenic role of *CSTB* as well as the potential underlying mechanisms in HCC through a series of in vitro experiments, such as CCK-8 assays, cloning assays, flow cytometry, Transwell assays, and western blotting. Our findings illustrated that the silencing of *CSTB* effectively suppressed cellular proliferation by inducing cell cycle arrest in the G2 phase and impaired HCC cell invasion and migration by stimulating epithelial-mesenchymal transition (EMT). Additionally, we analyzed the pathways enriched in HCC using RNA sequencing and found that the ERK/AKT/mTOR signaling pathway was related to increased *CSTB* expression in HCC. Finally, we confirmed the tumorigenic role of *CSTB* via in vivo experiments. Thus, our findings revealed that silencing *CSTB* inhibited the HCC progression via the ERK/AKT/mTOR signaling pathway, highlighting new perspectives for investigating the mechanisms of HCC.

1. Introduction

Primary liver carcinoma a prevalent malignant tumor worldwide, with Chinese patients accounting for approximately half of all liver cancer patients [1]. Among primary liver carcinoma cases, nearly 90 % are hepatocellular carcinoma (HCC) [2], a solid tumor with high proliferative, invasive, and metastatic potential and a poor overall survival rate [3]. Poor prognosis may also stem from early

* Corresponding author.
** Corresponding author. Institute of Aging, Key Laboratory of Alzheimer's Disease of Zhejiang Province, Zhejiang Provincial Clinical Research Center for Mental Disorders, School of Mental Health and Kangning Hospital, The Second Affiliated Hospital and Yuying Children's Hospital, Wenzhou Medical University, Wenzhou, Zhejiang 325000, China.
E-mail addresses: zwh@hospital.cqmu.edu.cn (W. Zhou), weihong@wmu.edu.cn (W. Song).

https://doi.org/10.1016/j.heliyon.2023.e23506
Received 13 August 2023; Received in revised form 14 November 2023; Accepted 5 December 2023
Available online 13 December 2023

metastasis, postoperative recurrence, and drug resistance [4]. While many studies have explored the mechanisms underlying HCC occurrence, recurrence, and metastasis [5,6], these mechanisms remain unclear. Therefore, it's crucial to understand the molecular mechanisms underlying HCC for enhancing the detection and therapy of liver cancer.

Cystatin B (*CSTB*) is to a member of family 1 (stefin), a cysteine protease inhibitor superfamily, and is encoded by the *CSTB* gene [7]. It hinders the function of different proteolytic enzymes, including cysteine proteases [8,9]. Previous studies have found that *CSTB* shows abnormal expression in several malignant neoplasms [10]. Specifically, the serum level of cystatin B is markedly higher in patients with liver carcinoma compared to those without liver cancer. Furthermore, HCC patients with elevated *CSTB* expression tend to relapse more often and have a shorter overall survival (OS) time [11]. These findings suggest that *CSTB* has potential as a prognostic indicator for HCC.

However, the mechanism through which *CSTB* promotes the progression of hepatocellular carcinoma and whether changes in *CSTB* gene expression affect the biological mechanism of HCC remain unclear and have not been reported. Therefore, we first confirmed through bioinformatics data analysis that *CSTB* expression was upregulated in HCC and connected to a poor OS rate. We then determined the tumorigenic role of *CSTB* through an array of tests. Additionally, our analysis identified the ERK/AKT/mTOR signaling pathway as being related to elevated *CSTB* expression in HCC. Collectively, the findings revealed a crucial role for *CSTB* in HCC and the related mechanisms, indicating that *CSTB* might be a key prognostic and treatment target for HCC patients.

2. Materials and methods

2.1. Data gathering

Analysis was conducted using download RNA-seq data from the TCGA-LIHC database of the Broad Institute (https://gdac.broadinstitute.org/) and a liver tumor dataset (GSE14520) was obtained from the GEO database (https://www.ncbi.nlm.nih.gov/geo/).

2.2. Gene expression, survival and Multivariate Cox regression analysis

The expression of the *CSTB* gene was analyzed using the limma R package. Prognosis assessment was carried out through the implementation of Kaplan–Meier curves and the survival package in R (version 4.1.3). Additionally, multivariate Cox regression analysis was conducted to evaluate the correlation between survival and *CSTB* gene expression, along with clinical and pathological characteristics that are associated with survival.

2.3. Cell lines

The HepG2 and SK-Hep-1 lines, human HCC cells, were obtained from ATCC (the American Type Culture Collection). They were cultured in Dulbecco's Modified Eagle Medium (DMEM, Gibco, Thermo, USA) with 10 % fetal bovine serum (FBS, ExCell Bio). The human hepatocyte cells THLE-2 (CTCC-004-0030) were purchased from the Meisen Chinese Tissue Culture Collections (MeisenCTCC) company (Zhejiang, China) and were cultured in THLE-2-CM (CTCC-002-046) from MeisenCTCC. To ensure optimal growth of THLE-2 cells, the culture dish was pre-coated with a unique coating medium (MeisenCTCC, CTCC-002-030) at least 24 h in advance. The culturing conditions of these cells were set at 37 °C, 95 % humidity, and a 5 % CO_2 atmosphere.

2.4. Lentivirus transfection

Lentiviral vectors encoding single guide RNAs (sgRNAs) targeting *CSTB* were constructed by Jikai (Shanghai, China). The sequences were as follows: LV-*CSTB*-sgRNA (Sg*CSTB*): CACCGAGTTTGTCCCCGCGACCAC; negative control sgRNA (SgNC): CGCTTCCGCGGCCCGTTCAA. The double-stranded DNA containing the interference sequences were synthesized and connected to the Lenti-CAS9-sgRNA-tag vector enhanced green fluorescent protein (EGFP, GV393). According to the specifications of the manufacturer, HCC cells were transfected with Sg*CSTB* and SgNC lentiviral vectors. Transfection efficiency was measured via western blotting. After a 2-week duration, transduced cells were selected with 2 μg/mL puromycin [12].

The CCK-8 assay initially involved $3x10^3$ cells per well in 96-well plates and 10 μl of Cell Counting Kit-8 (CCK-8, MCE, Shanghai, China) reagent was added to each well at the specified time points (0, 24, 48, 72, or 96 h). After a 2-h period of incubation, the cells absorbanceat a wavelength of 450 nm was measured. Regarding the colony formation experiment, each well of a 6-well plate initially contained 800 cells, followed by continuous cultivation for 2 weeks. To fix the cells, a 4 % paraformaldehyde solution was applied for 25 min. Subsequently, the cells were stained with crystal violet (Solarbio, Beijing, China) for 20 min.

2.5. Flow cytometric analysis

Cell cycle analysis was performed by seeding $1x10^6$ cells in each 6 cm dishes. The cells were harvested upon achieving 80 % confluency and fixed in 70 % ethanol for a minimum duration of 24 h at 4 °C. The fixed cells were centrifuged at 800 rpm for 10 min after undergoing two washes with PBS. Following this, incubation with a staining buffer, consisting of 100 μL of RNase A and 300 μL of propidium iodide (PI, Solarbio, Beijing, China), occurred in a dark room for 30 min. For flow cytometric analysis, $1x10^5$ cells per specimen were utilized.

2.6. Transwell migration and invasion assays

The determination of cell migration and invasion abilities was conducted using a polycarbonate insert featuring 8-μm pores (Corning, NY, USA) in 24-well plates. Initially, $1x10^5$ cells were positioned within each upper chamber, along with 300 μL of medium lacking serum. Subsequently, in the lower compartment, DMEM containing 30 % FBS was added. For the invasion assay, each upper chamber was pre-coated with 50 μL Matrigel (Becton Dickinson, USA) at least 24 h in advance. Following an incubation period of 48 h, the cells were fixed using 4 % paraformaldehyde for 25 min. Subsequently, the fixed cell and were stained with crystal violet (Solarbio, Beijing, China) for 20 min [13]. A minimum of five randomly chosen visual fields per chamber were assessed. The cell count in each field was conducted under a light microscope.

2.7. Western blotting

Total protein was extracted from HCC cells via RIPA lysis buffer (Beyotime, China) and was separated by 12.5 % sodium dodecyl sulfate–polyacrylamide gel electrophoresis (SDS–PAGE). Subsequently, the separated protein on the gel was immediately transferred to a polyvinylidene fluoride (PVDF) membrane (Millipore, USA) and blocked with 5 % milk. The membranes were incubated with primary antibodies at 4 °C overnight, included CSTB (ABclonal, A3815), cyclin B1 (Proteintech, 28603-1-AP), CDK1 (Proteintech, 19532-1-AP), CDC25C (Proteintech, 16485-1-AP), N-cadherin (Proteintech, 66219-1-Ig), vimentin (Proteintech, 60330-1-Ig), ERK (CST, 9102), *p*-ERK (CST, 4370), AKT (CST, 9272), *p*-AKT (CST, 9271), mTOR (CST, 2983), *p*-mTOR (CST, 5536), and GAPDH (Proteintech, 60004-1-Ig) antibodies. The visualization of protein bands was achieved using an enhanced chemiluminescence (ECL) kit.

2.8. mRNA sequencing analysis

For mRNA sequencing (RNAseq) analysis, two groups of HepG2 cells (SgNC and Sg*CSTB*) were inoculated in 10 cm dishes. Upon reaching 80 % confluence, the cells were subjected to TRIzol-based RNA isolation as the instructions and preserved at −80 °C. The quality and concentration of the total RNAs were measured by the Agilent 2100 Bioanalyzer and the RNA 6000 Nano kit (Agilent Technologies, USA). To purify mRNA, magnetic beads attached with oligo (dT) were employed, followed by fragmentation of the purified mRNA into smaller fragments. cDNA libraries suitable for sequencing were prepared and then sequenced via the PE150 platform of the MGI DNBSEQ-T7 system. Bioinformatics analysis was performed by Genetics Biotech (Chongqing, China).

2.9. Establishment of tumor xenografts in nude mice

In order to investigate the involvement of *CSTB* in neoplasm development in vivo, the study was conducted using male BALB/c athymic nude mice (Vitonglihe, N = 10) aged 4 weeks. The left forearm of each mouse was injected with a 100 μL solution of PBS containing either 4×10^6 SgNC-HepG2 (N = 5) cells or Sg*CSTB*-HepG2 (N = 5) cells. The mice were bred at the laboratory facility of Chongqing Medical University (Chongqing, China). Tumor formation in the nude mice was observed within 15 days, and the diameter of the tumor was measured via digital vernier calipers every two days from day 3 to day 15 after cell injection. Tumor volume was calculated as d^2 x D x 0.52 (mm^3), where d represents the shortest diameter and D refers the longest diameter. Ultimately, the mice were euthanized upon completion of the experiment [14,15].

2.10. Immunohistochemistry

Immunohistochemical (IHC) staining was performed as described previously [16]. The subcutaneous tumors of the sacrificed nude mice were removed and fixed with 4 % paraformaldehyde. Immunohistochemical staining of CSTB and Ki67, as well as H&E staining, was performed on paraffin-embedded sections measuring 4 μm in thickness. To ensure a representative sample, a total of five fields were randomly chosen and captured by a microscope at a magnification of 400 × .

2.11. Statistical analysis

R (4.1.3) packages were used for conducting statistical analysis and generating graphs. The Wilcoxon test was employed to analyze differences between groups, while Spearman analysis of the bioinformatics data was used to examine correlations. The data are presented as the mean ± SD of a minimum of three independent trials. Statistical analysis was conducted by employing the GraphPad Prism 8.0 software (San Diego, USA). To evaluate variations among the different groups, either Student's t-test or one-way ANOVA was employed, and $p < 0.05$ was considered significant.

3. Results

3.1. CSTB is Highly expressed in liver hepatocellular carcinoma (LIHC) and related to poor prognosis in patients with LIHC

We examined the levels of *CSTB* in LIHC and neighboring normal tissues in the GSE14520 dataset. It was found that *CSTB* expression levels were obviously higher in cancerous tissues ($p < 0.001$) (Fig. 1A). Additionally, increased *CSTB* protein expression

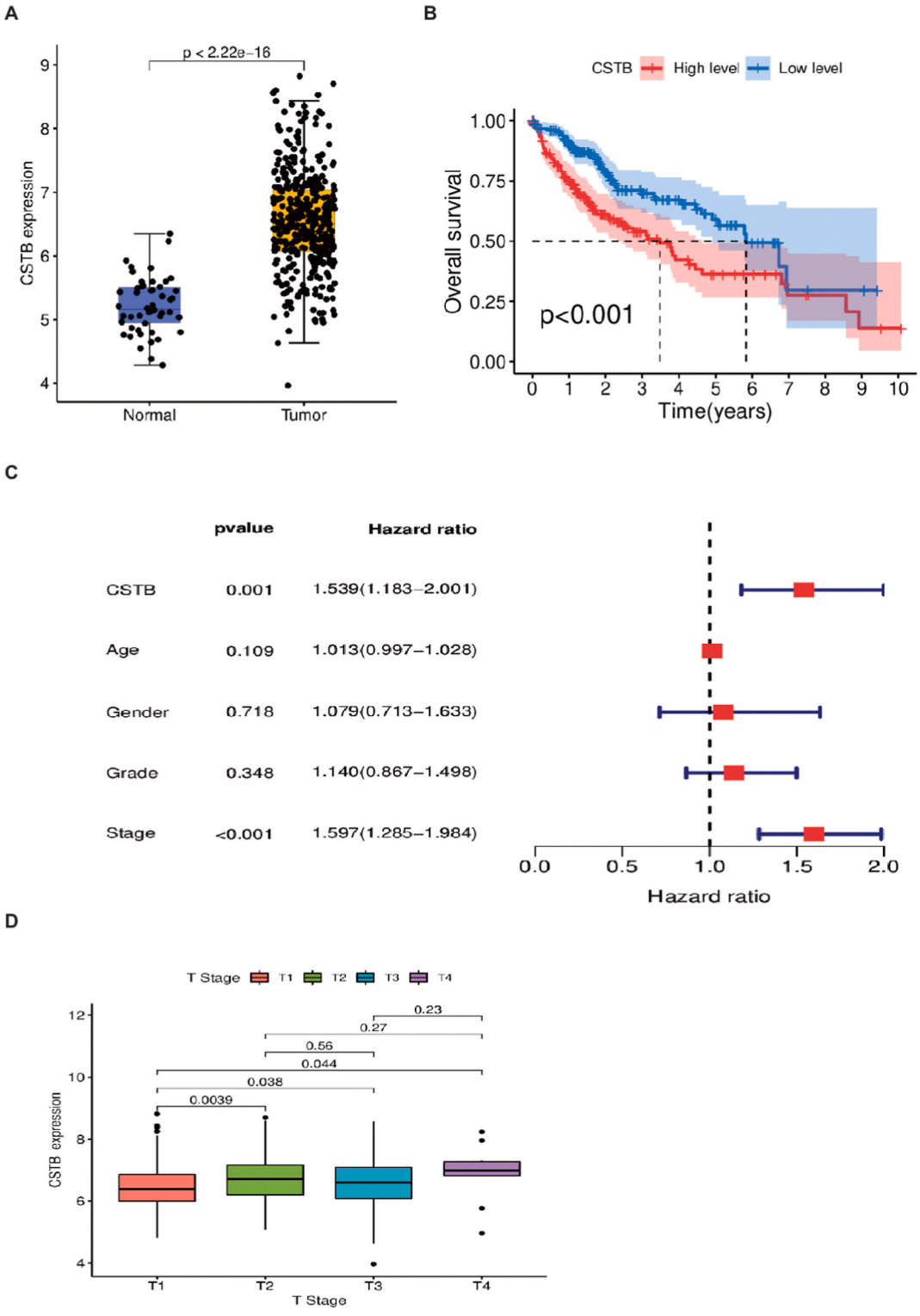

Fig. 1. *CSTB* expression in LIHC and adjacent normal tissues. (A) *CSTB* expression levels in the TCGA-LIHC dataset. (B) Kaplan–Meier analysis assessing the associated between survival and *CSTB* expression in the TCGA dataset. (C) Multivariate Cox regression results visualized in a forest plot. HR, hazard ratio. (D) The correlation between *CSTB* expression and clinical factors (T stage) in LIHC. The p-value for the difference between the factors is shown above the boxplot. (*p < 0.05, **p < 0.01, ***p < 0.001).

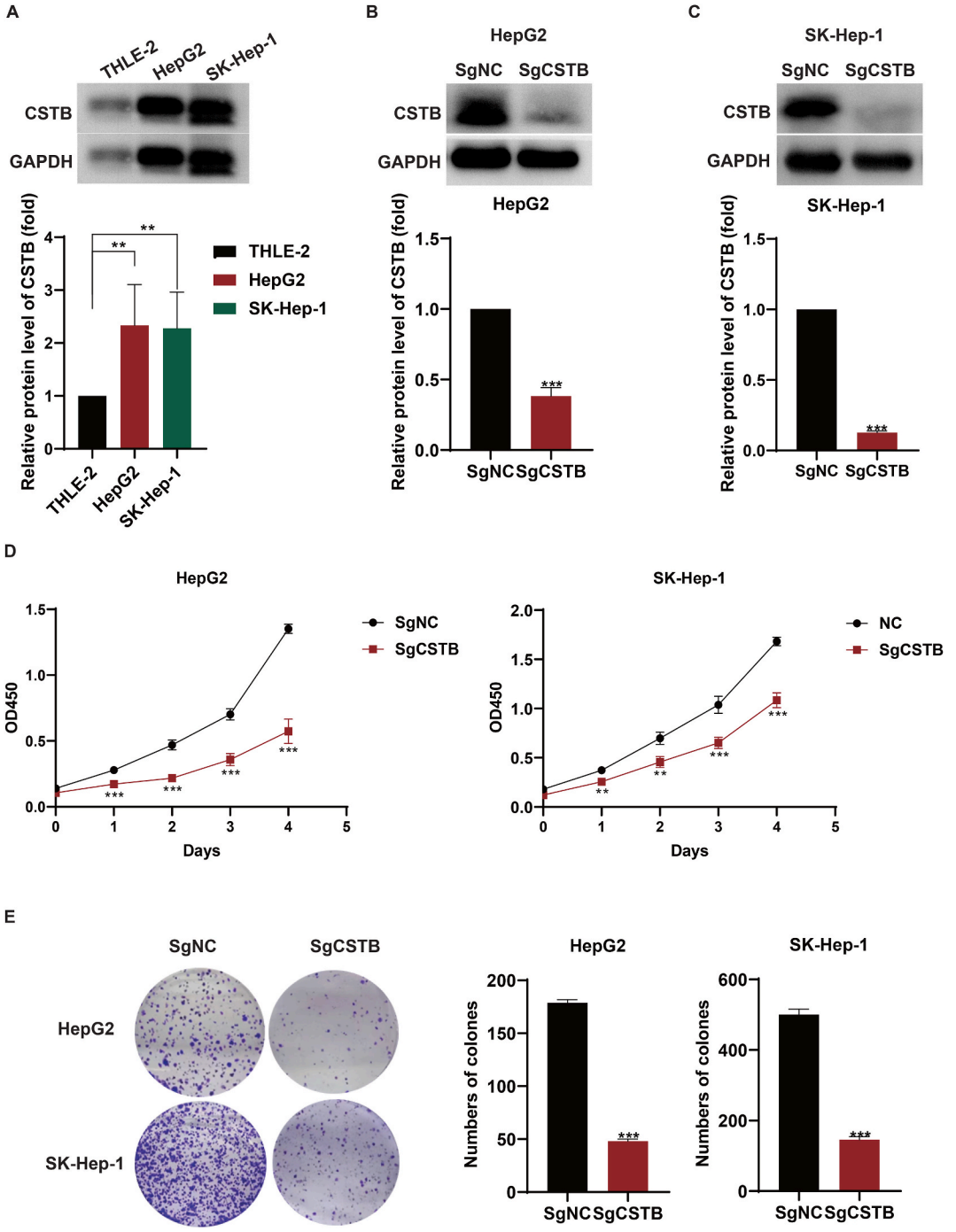

Fig. 2. The suppression of *CSTB* impeded the growth, motility, and invasiveness of HCC cells. (A) The protein expression of *CSTB* in one type of hepatocyte cell (THLE-2) and two types of HCC cells (HepG2 and SK-Hep-1). The representative images (above) and quantitative data (below) are presented. Uncropped gels and blots refer to Fig. S1 in supplementary material. (B, C) The protein levels of *CSTB* in stable cell lines via western blotting. GAPDH was used as an internal control. The representative images (above) and quantitative data (below) are presented. Uncropped gels and blots refer to Fig. S4 in supplementary material. (D) Growth curves of HCC cells tested by the CCK-8 assay. (E) The colony formation assay of different groups of HCC cells. Colonies containing at least 50 cells were enumerated, and the efficiency of colony formation was calculated. The representative images (left) and quantitative data (right) are presented. (*$p < 0.05$, **$p < 0.01$, ***$p < 0.001$).

levels were detected in HepG2 (3.50 ± 1.46, $p < 0.05$) and SK-Hep-1 (3.25 ± 1.27, $p < 0.05$) cells compared to THLE-2 cells by western blotting (Fig. 2A). In addition, we examined the association between OS and *CSTB* expression in the TCGA cohort via Kaplan–Meier analysis. The findings revealed that elevated *CSTB* expression was obviously related to poorer OS in LIHC patients ($p < 0.001$) (Fig. 1B). We speculated that *CSTB* expression levels were related to poor prognostic outcomes in LIHC patients.

3.2. CSTB was an independent prognostic factor for LIHC

To explore the potential role of *CSTB* as an independent prognostic marker in individuals diagnosed with LIHC, we conducted a comprehensive multivariate analysis. This analysis encompassed the evaluation of *CSTB* expression, as well as gender, age, tumor stage and grade. In the TCGA cohort, multivariate Cox regression analysis revealed that *CSTB* expression (HR, 1.539; 95 % CI, 1.183–2.001; $p < 0.001$) and tumor stage (HR, 1.597; 95 % CI, 1.285–1.984; $p < 0.001$) were identified as independent factors predicting prognosis for LIHC (Fig. 1C). The results demonstrated the prognostic significance of *CSTB* expression in LIHC. Overall, these findings demonstrated the potential of *CSTB* as an independent prognostic biomarker in LIHC patients.

3.3. Correlation between CSTB expression and clinical factors in LIHC based on the TCGA database

In order to examine the correlation between clinical variables and *CSTB* expression, an investigation was conducted on the

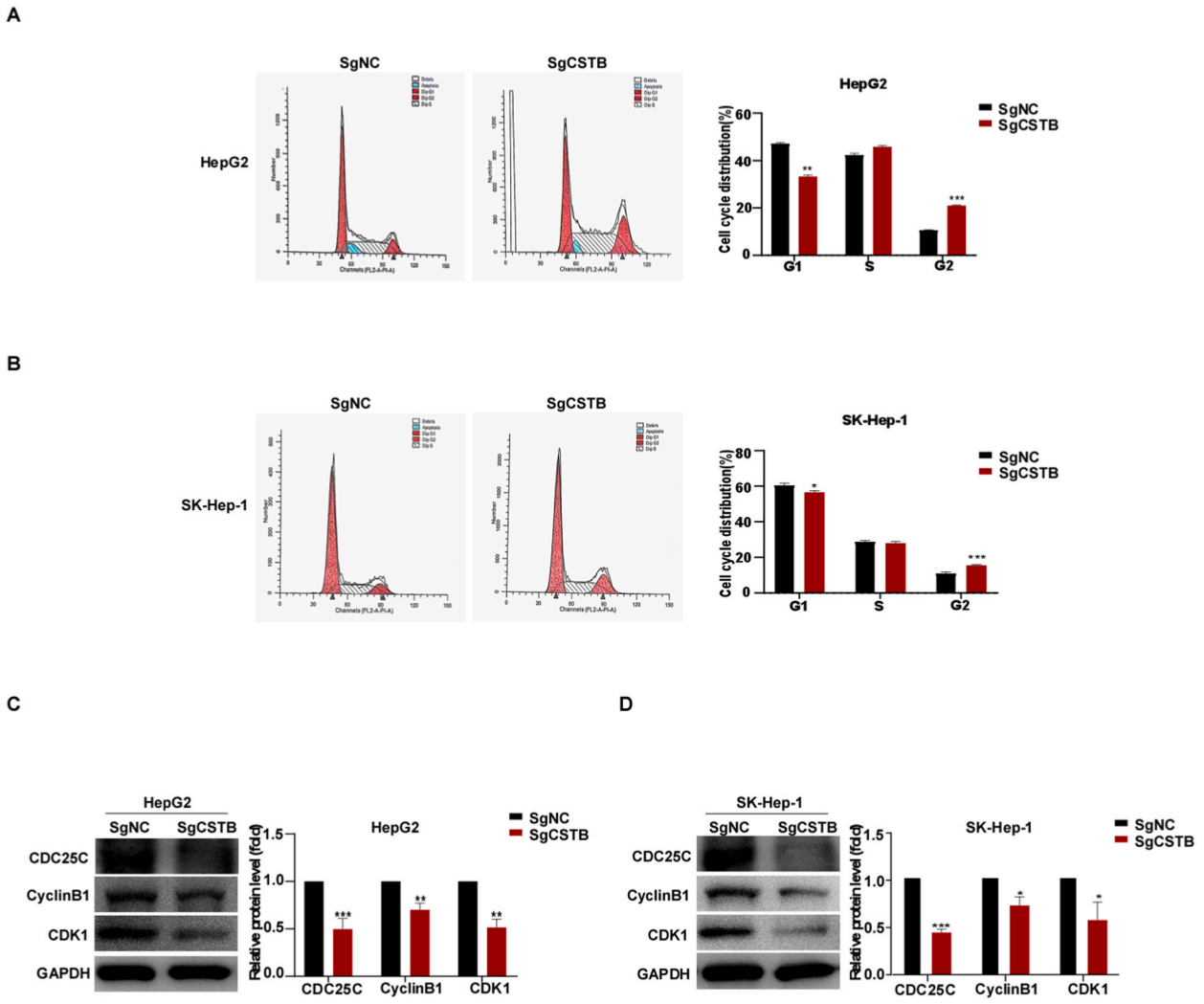

Fig. 3. The silencing of *CSTB* resulted in the arrest of hepatocellular carcinoma cells during the G2 phase. (A, B) Flow cytometry analysis performed to assess the distribution of the cell cycle in different groups of HCC cells. (C, D) Protein levels of Cyclin B1, CDK1, and CDC25C in HCC cells of control (NC) group and the *CSTB*-silenced group. GAPDH served as the internal control. Uncropped gels and blots refer to Fig. S2 in supplementary material. Representative images (left) and quantitative data (right) are presented. (*$p < 0.05$, **$p < 0.01$, ***$p < 0.001$).

relationship of *CSTB* with tumor stage in LIHC. The findings clearly demonstrated a marked elevation in *CSTB* expression in the T2 to T4 stages ($p < 0.05$) compared to the T1 stage ($p < 0.05$) (Fig. 1D). Additionally, *CSTB* expression exhibited a strong association with the invasion of HCC cells into surrounding structures and was the primary determinant of tumor stage, implying patients with advanced hepatic tumors showed higher levels of *CSTB* expression.

3.4. Silencing CSTB expression inhibited HCC proliferation

After the transfection of *CSTB* sgRNA and control sgRNA into HepG2 and SK-Hep-1 cells, it was verified that the *CSTB* protein expression was apparently downregulated in the sg*CSTB* group comparing to the sgNC group ($p < 0.001$) through western blotting and the *CSTB*-silenced cell lines were successfully established (Fig. 2B and C). Next, the CCK-8 assay proved that the cell proliferation rate was markedly reduced after silencing of *CSTB* ($p < 0.01$) (Fig. 2D). Additionally, colony formation assays revealed a remarkable inhibition of colony formation after *CSTB* silencing ($p < 0.01$) (Fig. 2E), aligning with the outcomes of the CCK-8 assay.

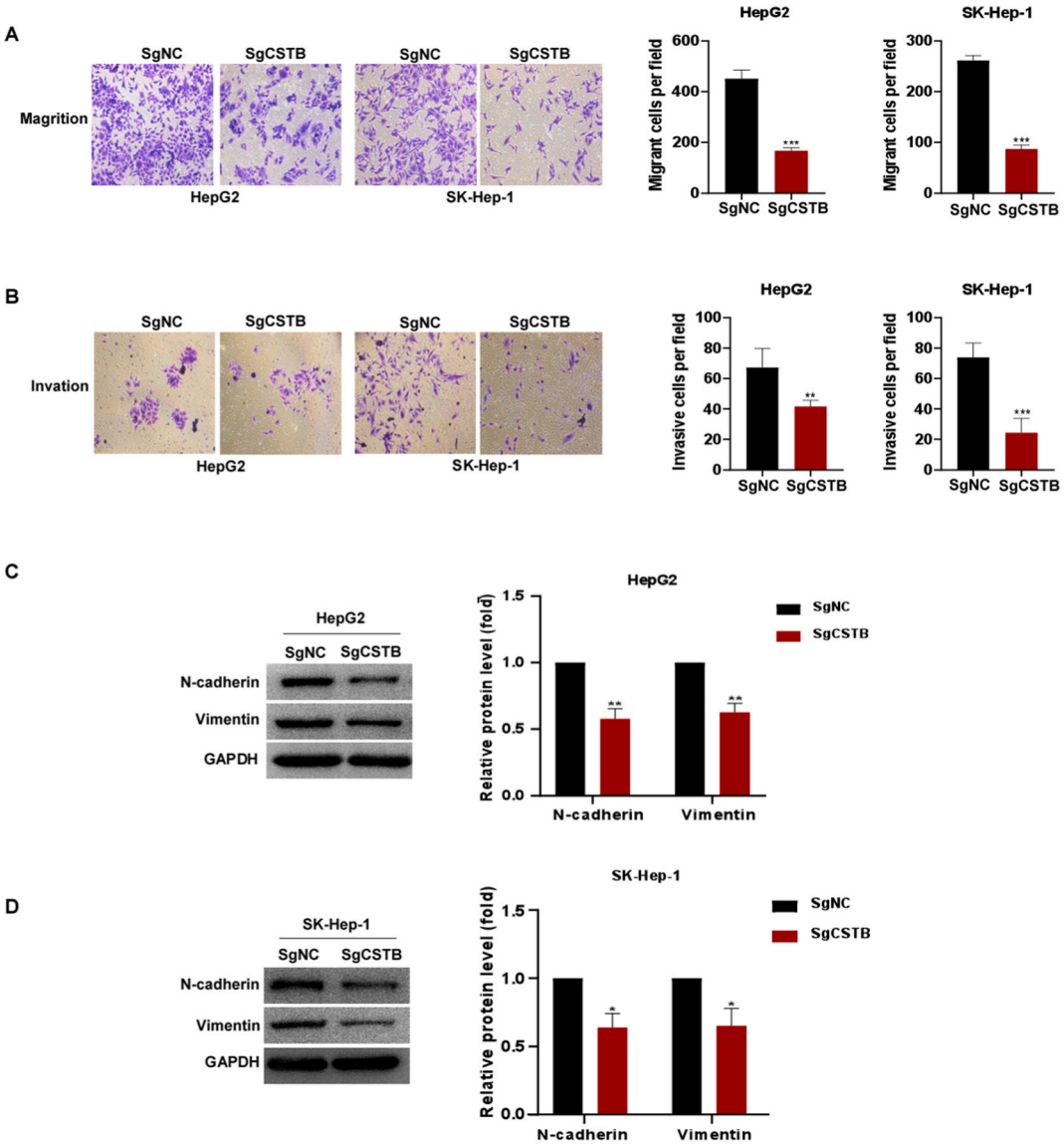

Fig. 4. Silencing *CSTB* inhibited the migration and invasion of hepatocellular carcinoma cells. (A, B) Cell migration and invasion abilities analyzed by the Transwell migration assay. (C, D) The protein levels of N-cadherin and vimentin in HCC cells of control (NC) group and the *CSTB*-silenced group. GAPDH is served as the internal control. Uncropped gels and blots refer to Fig. S3 in supplementary material. Representative images (left) and quantitative data (right) are shown (*$p < 0.05$, **$p < 0.01$, ***$p < 0.001$).

3.5. CSTB silencing induced arrest of HCC cells in G2 stage

In order to delve deeper into the biological significance of *CSTB* in HCC, we assessed the impact of *CSTB* on the cell cycle in HCC cells. Flow cytometry analysis results showed that *CSTB* silencing led to cell cycle arrest at the G2 phase, as the number of HepG2 cells

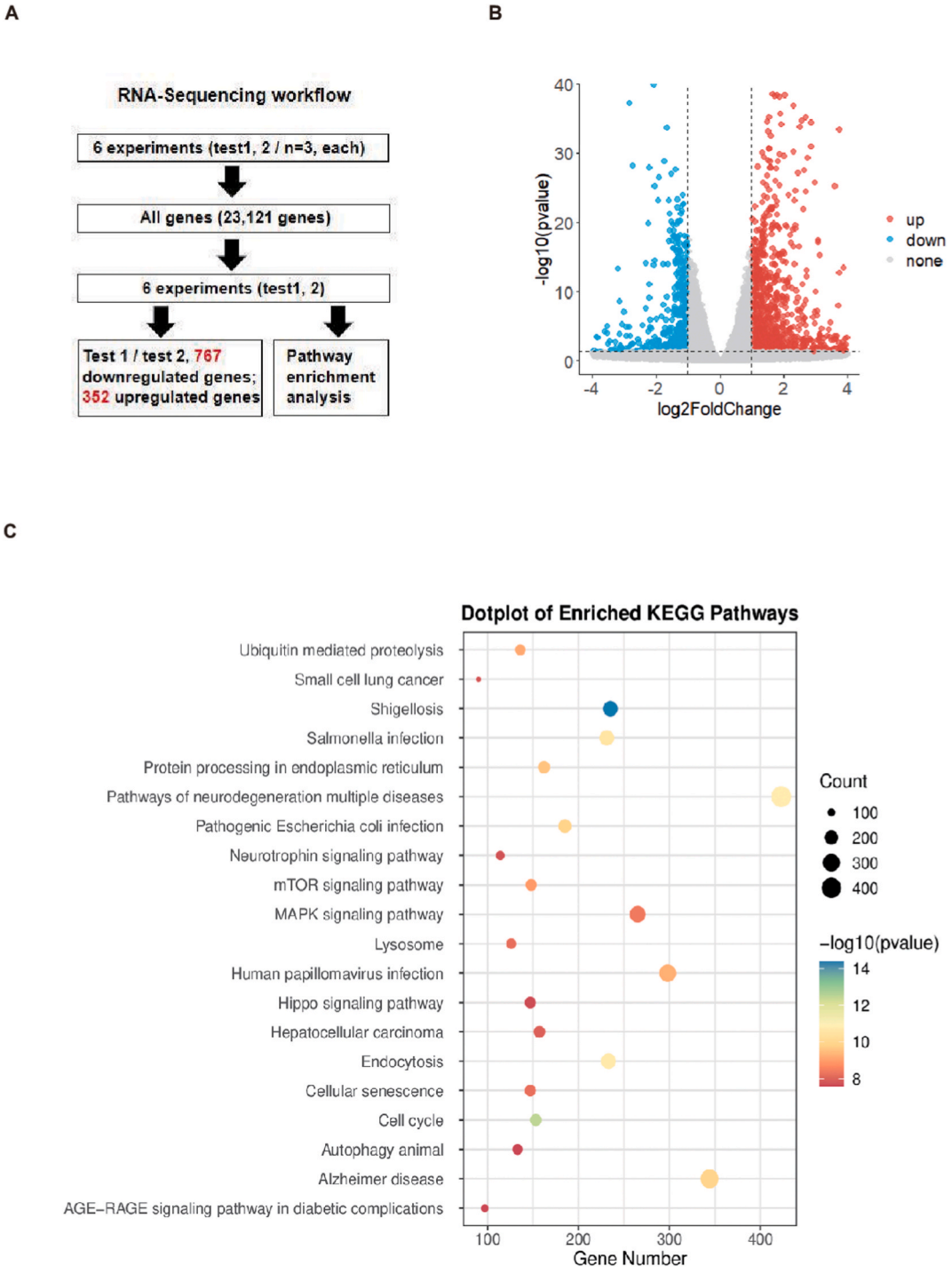

Fig. 5. KEGG analysis of DEGs identified by RNA-seq. (A) Workflow of the RNA-seq experiment and (B) volcano map of the DEGs. In the volcano map, red dots indicate genes that have experienced upregulation, whereas blue dots represent genes that have undergone downregulation. (C) The mTOR and MAPK pathways were significantly enriched for the DEGs related to HCC progression in the presence of different levels of *CSTB*. (For interpretation of the references to colour in this figure legend, the reader is referred to the Web version of this article.)

(20.95 ± 0.23 %, compared to 10.55 ± 0.25 %, $p < 0.001$) (Fig. 3A) and SK-Hep-1 cells (15.51 ± 0.336 %, compared to 10.91 ± 0.76 %, $p < 0.001$) in G2 phase was increased (Fig. 3B). Additionally, the protein expression levels of cyclin B1 (0.70 ± 0.12, $p < 0.01$), CDK1 (0.51 ± 0.15, $p < 0.01$) and CDC25C (0.50 ± 0.25, $p < 0.001$), which are involved in mitotic progression, were decreased in *CSTB*-silenced HepG2 cells compared with NC cells (Fig. 3C and D). Similarly, cyclin B1 (0.71 ± 0.15, $p < 0.05$), CDK1 (0.56 ± 0.32, $p < 0.05$) and CDC25C (0.43 ± 0.06, $p < 0.001$) expression levels were reduced after silencing of *CSTB* in SK-Hep-1 cells (Fig. 3C and D).

3.6. *CSTB silencing inhibited HCC migration and invasion through EMT*

The functional role of *CSTB* in cell migration and invasion was assessed in depth. The research findings demonstrated a notable decrease in hepatocellular carcinoma cell migration following *CSTB* silencing, as comparing to the control group ($p < 0.01$) (Fig. 4A and B). The western blotting results revealed that *CSTB* silencing decreased the expression of N-cadherin (0.58 ± 0.13, $p < 0.01$) and vimentin (0.63 ± 0.11, $p < 0.01$) in HepG2 cells (Fig. 4C and D). In addition, N-cadherin (0.64 ± 0.18, $p < 0.05$) and vimentin (0.65 ± 0.22, $p < 0.05$) expression levels were reduced after silencing of *CSTB* in SK-Hep-1 cells (Fig. 4C and D). These findings identified the influence of *CSTB* on the expression of EMT proteins, but the specific mechanism needs further exploration.

3.7. *CSTB silencing inhibited the progression of HCC by suppressing the ERK/AKT/mTOR pathway*

Based on the above in vitro experiments, we analyzed the potential mechanism underlying the role of *CSTB* in HCC by RNA-seq (Fig. 5A). Gene expression levels were determined using Salmon (v1.4.0) after mapping the FASTQ reads to the human genome

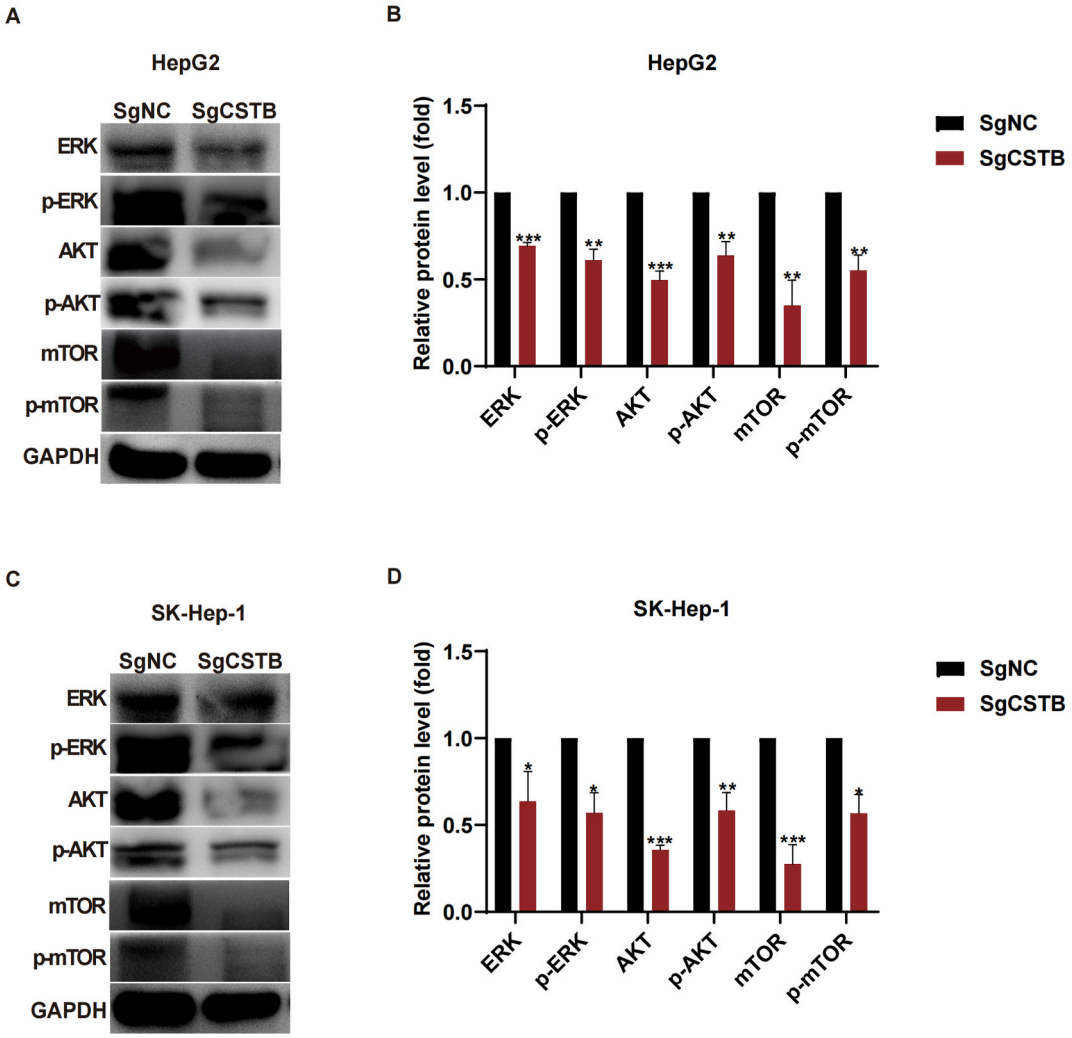

Fig. 6. Silencing *CSTB* inhibited the activation of the ERK/Akt/mTOR signaling pathway. The protein levels of ERK, *p*-ERK, AKT, *p*-AKT, mTOR, and *p*-mTOR in (A, B) HepG2 and (C, D) SK-Hep-1 cells. GAPDH was utilized as an internal standard. Representative images (left) and quantitative data (right) are shown (*$p < 0.05$, **$p < 0.01$, ***$p < 0.001$). Uncropped gels and blots refer to Fig. S4 in supplementary material.

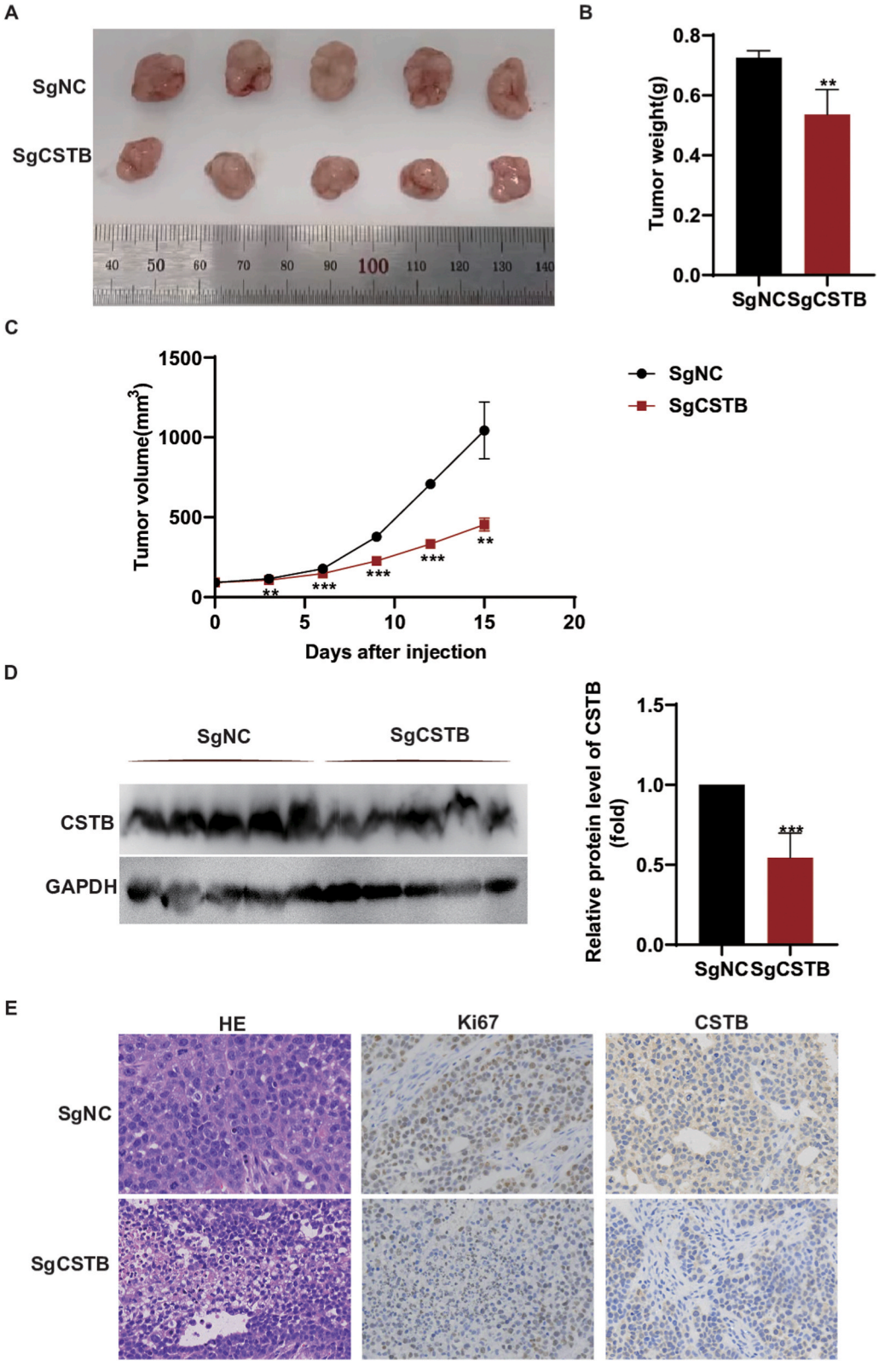

(caption on next page)

Fig. 7. Silencing *CSTB* inhibited tumor growth in vivo. (A) Tumors captured from distinct groups of mice. (B) Analysis of tumor weight among mice conducted through statistical means. (C) Tumor growth curve representing each group of mice. (D) *CSTB* protein expression in tumor tissues. GAPDH was utilized as an internal control. Representative images (left) and quantitative data (right) are shown. Uncropped gels and blots refer to Fig. S5 in supplementary material. (E) IHC staining of CSTB and ki67 and HE staining of tumor tissues. (**p < 0.01, ***p < 0.001).

(GRCh38.p14) through HISAT2 (v2.0.4). We identified 1519 differentially expressed genes (DEGs) in *CSTB*-silenced HepG2 cells compared to NC cells, including 989 upregulated and 530 downregulated genes (Fig. 5B). DEGs were identified based on an absolute fold change greater than 1 and a p-value lower than 0.05. Next, we conducted an examination using Kyoto Encyclopedia of Genes and Genomes (KEGG) pathway analysis to determine the pathways linked to the transcripts displaying differential expression. The assessment of gene expression variation was conducted using the limma R package. The outcomes obtained from the KEGG pathway analysis demonstrated that the association between *CSTB* and HCC involves significant contributions from both the MAPK and mTOR signaling pathways (Fig. 5C).

Afterwards, the protein levels of certain crucial molecules related to mTOR signaling were assessed. The expression of AKT (0.50 ± 0.09, $p < 0.001$), *p*-AKT (0.64 ± 0.18, $p < 0.001$), mTOR (0.35 ± 0.32, $p < 0.01$), *p*-mTOR (0.55 ± 0.15, $p < 0.01$), ERK (0.69 ± 0.04, $p < 0.001$) and *p*-ERK (0.61 ± 0.11, $p < 0.01$) (Fig. 6A and B) was reduced in *CSTB*-silenced HepG2 cells compared to negative control HepG2 cells. Similarly, the expression of AKT (0.37 ± 0.04, $p < 0.001$), *p*-AKT (0.58 ± 0.23, $p < 0.001$), mTOR (0.28 ± 0.25, $p < 0.01$), *p*-mTOR (0.57 ± 0.19, $p < 0.05$), ERK (0.64 ± 0.30, $p < 0.05$) and *p*-ERK (0.57 ± 0.20, $p < 0.05$) in SK-Hep-1 cells (Fig. 6C and D) were downregulated after the silencing of *CSTB*. These findings suggested that *CSTB* silencing might inhibit HCC cellular progression by suppressing ERK/AKT/mTOR signaling.

3.8. Silencing CSTB inhibited xenograft tumor growth In vivo

To further investigate the inhibitory effect of *CSTB* silencing on tumor growth, we employed a xenograft model in mice. In this experiment, the sg*CSTB* group demonstrated a significant hindrance to the growth of the xenografts, as compared to the sgNC group ($p < 0.001$, Fig. 7A). Moreover, the mean weight of the neoplasms was notably ($p < 0.001$, Fig. 7B) lower in the Sg*CSTB* group (0.1 ± 0.05 g) compared to the SgNC group (0.3 ± 0.05 g). As illustrated in Fig. 7C, the volume of the tumors in the Sg*CSTB* group was measured 128.3 ± 47.7 mm^3, whereas it was 498.5 ± 142.9 mm^3 in the SgNC group. Furthermore, the *CSTB* protein expression level in the Sg*CSTB* group was lower than that of the SgNC group ($p < 0.001$, Fig. 7D). The IHC staining results of HCC xenograft tissues demonstrated a significant decrease of CSTB and Ki67 protein expression levels after *CSTB* silencing (Fig. 7E). These findings demonstrated the antitumor impact of *CSTB* gene suppression on HCC cells within nude mice.

4. Discussion

The process of HCC tumorigenesis is intricate and encompasses various factors, leading to an escalating global incidence of HCC-related mortality. Although great improvements have been made in the treatment of HCC, tools for predicting the relapse and metastasis rates of HCC patients after surgery are lacking. Previous studies [17–20] have revealed that various molecules play key roles in HCC development and progression, providing evidence for the value of potential target molecules for HCC diagnosis and therapy. A previous study [11] highlighted the elevation of *CSTB* in HCC tissues. Nonetheless, the biological role of *CSTB* in HCC and its corresponding molecular mechanisms have yet to be fully elucidated. Thus, the objective of this research is to delve into the unknown mechanisms underlying *CSTB*'s involvement in HCC tumor formation and advancement.

Through the analysis of bioinformatics data, we initially discovered the notably elevated *CSTB* expression levels in LIHC tissues comparing to the adjacent normal tissues. Moreover, *CSTB* expression levels were connected to poor prognostic outcomes in patients with LIHC and high *CSTB* levels were also associated with a higher T stage in HCC patients. The results of several in vitro assays demonstrated that silencing *CSTB* could evidently impede the migration, invasion and proliferation of HCC cells, implying the potential of *CSTB* as an oncogene in hepatocellular carcinoma. Subsequent in vivo studies in which the expression of Ki67, widely used in cancer biology as a marker of tumor cell proliferation, was analyzed also illustrated that *CSTB* silencing prevented HCC cells from proliferating [21]. This findings were consistent with other studies; for example, it was observed that inhibiting *CSTB* expression in a cell line of epithelial ovarian cancer led to a limitation in cellular growth [22].

To further determine the pathway via which *CSTB* promotes tumor growth, cell cycle analysis was conducted. Our findings revealed that silencing *CSTB* resulted in the arrest of HCC cells in the G2 phase. The progression of the cell cycle in eukaryotes is regulated by a complex system that involves the tight control of cyclin-dependent kinases (CDKs). Cyclins can activate diverse CDKs to accelerate cell cycle progression. For instance, the main role of cyclin B1 is controlling the progression of cells from G2 phase to M phase [23–26]. Once cells enter the prophase, the activity of cyclin B1-CDK1 is enhanced [27]. Subsequently, the activated cyclin B1-CDK1 complex translocates to the nucleus, thereby expediting cellular division [28]. Additionally, the vital function of cell division cycle 25C (CDC25C) is to facilitate the G2/M transition of mitotic cells through the modulation of serine/threonine kinases' activity and initiation of CDK1 dephosphorylation to activate the cyclin B1/CDK1 complex [29,30]. Thus, to understand how *CSTB* triggers G2 arrest in depth, CDC25C, cyclin B1 and CDK1 protein expression were examined. Our results proved that *CSTB* arrested cells in G2 phase by restraining the CDC25C/CDK1/CyclinB1 pathway using flow cytometry and western blotting.

Invasion and metastasis are critical in the mechanisms underlying cancer-related deaths, especially in HCC [31]. They are also multistep and intricate processes controlled by various genes related to tumor adhesion, matrix degradation and tumor cellular

migration [32]. Epithelial-mesenchymal transition (EMT) is a pivotal factor contributing to the advancement of cancer, bringing about a more metastatic and aggressive phenotype in tumors [33]. At the molecular level, EMT is closely associated with an array of processes involving mesenchymal and epithelial markers. Previously researches have proposed a close association between the recurrence and metastasis of liver carcinoma and EMT [34]. Therefore, we investigated the protein expression levels of EMT markers in HCC cells and revealed a noticeable reduction of them in HCC cells after *CSTB* silencing. This finding indicated that HCC migration may be controlled by *CSTB* via EMT. According to the report, alongside causing G2M phase arrest in HCC, the repression of CyclinB1 also hampered EMT by restricting the manifestation of N-cadherin and vimentin [35]. Accordingly, we conjectured that the CDC25C/CDK1/cyclin B1 pathway may be responsible for the suppression of EMT after *CSTB* silencing.

The RNA-seq results showed that *CSTB* was associated with many mechanisms related to the MAPK pathway, ubiquitin-mediated proteolysis, the mTOR signaling pathway, the Hippo signaling pathway, and the cell cycle (Fig. 5C). Prior researches have indicated that the AKT/mTOR pathway has a crucial function in the development of malignant tumors, including cell proliferation and migration processes [36–39]. Additionally, many studies have validated the involvement and crucial role of the AKT/mTOR pathway in HCC [40–42]. Additionally, *CSTB* has been demonstrated to partake in the progression of certain malignant tumors by affecting the AKT/mTOR signaling pathway [43]. In the realm of HCC-related signaling pathways, the MAPK/ERK signaling pathway stands out as one of the most pivotal pathways in the development of HCC [44]. Moreover, the mRNA level of ERK was evidently decreased after cystatin B-like (CSTB-L) silencing, indicating the potential positive role of CSTB-L in the antiviral immune response via the MAPK/ERK pathway [45]. Basing on these findings, RNA-seq results were considered to thoroughly explore the impact of *CSTB* on the MAPK and mTOR signaling pathways in HCC. Our research revealed that *CSTB* knockdown significantly restrained the activation of the ERK/AKT/mTOR signaling pathway.

According to previous research studies, it has been observed that AKT1 has the ability to bind to vimentin at serine 39, which consequently hinders its proteolysis, thus promoting tumor metastasis and growth [46]. Another study has identified that the second coiled-coil domain within Vimentin is implicated in the tumorigenic pathway associated with ERK, functioning through the interaction with phosphorylated ERK [47]. From these findings, a hypothesis was formulated that the inhibition of *CSTB* could potentially hinder the migration and invasion of HCC cells. Additionally, previous study has demonstrated that the cell cycle regulation involves the PI3K-AKT signaling pathway [48,49]. Furthermore, the translocation of cyclin B1 to the nucleus has been attributed to ERK, which phosphorylates the cytoplasmic retention sequence necessary for the nuclear localization and mitotic progression of cyclin B1 [50]. Thus, suppression of ERK activity results in the cytoplasmic retention of the cyclin B/Cdc2 complex, causing a delay in mitosis. From these findings, it can be speculated that silencing *CSTB* may induce cell cycle arrest and impede cellular migration and invasion by inhibiting the ERK/AKT/mTOR signaling pathway.

Undoubtedly, our research had several limitations. The absence of a negative control group containing untreated cells in cell-based assays and naive tumor cells without sgNC transduction in mice experiments, which reduced the rigor of this research to some extent but should have minimal impact on the overall conclusions. Additonally, in-depth exploration is required to determine whether the overexpression of *CSTB* in HCC can promote cellular proliferation and invasion. Furthermore, the precise role of *CSTB* in modulating the ERK/AKT/mTOR pathway in HCC is still ambiguous and necessitates further investigation. Recent studies have shown that single-cell sequencing and multiomic methods can be used to accurately analyze the complex biological systems of tumors [51,52]. Therefore, applying single-cell sequencing and multiomic approaches might provide comprehensive insights into the role of *CSTB* in HCC at the molecular level.

5. Conclusions

In conclusion, we validated that *CSTB* accelerates the progression of HCC by affecting the proliferation, invasion and metastasis of HCC cells. Based on previous studies, we further explored the underlying mechanism and found that *CSTB* inhibition exerted suppressive effects on HCC cells via the ERK/AKT/mTOR signaling pathway, which revealed the potential mechanisms and provided novel perspectives for the role and function of *CSTB* in HCC.

Funding

The National Natural Science Foundation of China (Grant No.81571388).

Ethics approval and consent to participate

This study was approved by the Ethics Committee of the Children's Hospital of Chongqing Medical University (Approval number: CHCMU-IACUC20230717003, Chongqing, China).

CRediT authorship contribution statement

Weiyi Zhu: Writing - review & editing, Writing - original draft, Software, Resources, Methodology, Formal analysis, Data curation. **Xiangjun Dong:** Writing - review & editing, Methodology. **Na Tian:** Methodology. **Zijuan Feng:** Software, Methodology. **Weihui Zhou:** Writing - review & editing, Methodology, Conceptualization. **Weihong Song:** Project administration, Funding acquisition, Conceptualization.

Declaration of competing interest

The authors declare that they have no known competing financial interests or personal relationships that could have appeared to influence the work reported in this paper.

Acknowledgments

This work was supported by the Graduate Student Research Innovation Project of Chongqing.

Appendix A. Supplementary data

Supplementary data to this article can be found online at https://doi.org/10.1016/j.heliyon.2023.e23506.

References

[1] M. Tanaka, et al., Hepatitis B and C virus infection and hepatocellular carcinoma in China: a review of epidemiology and control measures, J. Epidemiol. 21 (6) (2011) 401–416.
[2] J. Ferlay, et al., Cancer incidence and mortality worldwide: sources, methods and major patterns in GLOBOCAN 2012, Int. J. Cancer 136 (5) (2015) E359–E386.
[3] K. Mazmishvili, et al., Study to evaluate the immunomodulatory effects of radiofrequency ablation compared to surgical resection for liver cancer, J. Cancer 9 (17) (2018) 3187–3195.
[4] A. Colecchia, et al., Prognostic factors for hepatocellular carcinoma recurrence, World J. Gastroenterol. 20 (20) (2014) 5935–5950.
[5] T. Clark, et al., Hepatocellular carcinoma: review of epidemiology, screening, imaging diagnosis, response assessment, and treatment, Curr. Probl. Diagn. Radiol. 44 (6) (2015) 479–486.
[6] Y. Tamai, et al., The prognostic role of controlling nutritional status and skeletal muscle mass in patients with hepatocellular carcinoma after curative treatment, Eur. J. Gastroenterol. Hepatol. 34 (12) (2022) 1269–1276.
[7] V. Turk, W. Bode, The cystatins: protein inhibitors of cysteine proteinases, FEBS Lett. 285 (2) (1991) 213–219.
[8] D. Keppler, Towards novel anti-cancer strategies based on cystatin function, Cancer Lett. 235 (2) (2006) 159–176.
[9] V. Turk, V. Stoka, D. Turk, Cystatins: biochemical and structural properties, and medical relevance, Front. Biosci. 13 (2008) 5406–5420.
[10] N. Levicar, et al., Comparison of potential biological markers cathepsin B, cathepsin L, stefin A and stefin B with urokinase and plasminogen activator inhibitor-1 and clinicopathological data of breast carcinoma patients, Cancer Detect. Prev. 26 (1) (2002) 42–49.
[11] M.J. Lee, et al., Identification of cystatin B as a potential serum marker in hepatocellular carcinoma, Clin. Cancer Res. 14 (4) (2008) 1080–1089.
[12] P.H. Zhou, et al., Lentivirus-mediated RASSF1A expression suppresses aggressive phenotypes of gastric cancer cells in vitro and in vivo, Gene Ther. 22 (10) (2015) 793–801.
[13] X. Wang, et al., CYT387, a potent IKBKE inhibitor, suppresses human glioblastoma progression by activating the Hippo pathway, J. Transl. Med. 19 (1) (2021).
[14] J.-H. Seo, E.-S. Jeong, Y.-K. Choi, Therapeutic effects of lentivirus-mediated shRNA targeting of cyclin D1 in human gastric cancer, BMC Cancer 14 (1) (2014).
[15] J.-H. Park, et al., p>Lentivirus-Mediated VEGF knockdown suppresses gastric cancer cell proliferation and tumor growth in vitro and in vivo</p>, OncoTargets Ther. 13 (2020) 1331–1341.
[16] C.B. Del Debbio, et al., Notch signaling activates stem cell properties of muller glia through transcriptional regulation and skp2-mediated degradation of p27Kip1, PLoS One 11 (3) (2016), e0152025.
[17] S.A. Sharma, et al., Toronto HCC risk index: a validated scoring system to predict 10-year risk of HCC in patients with cirrhosis, J. Hepatol.68 1 (2017) 92–99.
[18] M. Frau, et al., Prognostic markers and putative therapeutic targets for hepatocellular carcinoma, Mol. Aspect. Med. 31 (2) (2010) 179–193.
[19] Y. Qu, et al., FYB2 is a potential prognostic biomarker for hepatocellular carcinoma, Liver 2 (4) (2022) 361–371.
[20] H. Wang, et al., LINC01468 drives NAFLD-HCC progression through CUL4A-linked degradation of SHIP2, Cell Death Dis. 8 (1) (2022) 449.
[21] A. Soares, et al., Novel application of Ki67 to quantify antigen-specific in vitro lymphoproliferation, J. Immunol. Methods 362 (1–2) (2010) 43–50.
[22] Y.Y. Lin, et al., Tissue levels of stefin A and stefin B in hepatocellular carcinoma, Anat. Rec. 299 (4) (2016) 428–438.
[23] J. Massague, G1 cell-cycle control and cancer, Nature 432 (7015) (2004) 298–306.
[24] D. Coverley, H. Laman, R.A. Laskey, Distinct roles for cyclins E and A during DNA replication complex assembly and activation, Nat. Cell Biol. 4 (7) (2002) 523–528.
[25] R.O. Adeyemi, D.J. Pintel, Parvovirus-induced depletion of cyclin B1 prevents mitotic entry of infected cells, PLoS Pathog. 10 (1) (2014), e1003891.
[26] M. Jackman, et al., Active cyclin B1-Cdk1 first appears on centrosomes in prophase, Nat. Cell Biol. 5 (2) (2003) 143–148.
[27] O. Gavet, J. Pines, Progressive activation of CyclinB1-Cdk1 coordinates entry to mitosis, Dev. Cell 18 (4) (2010) 533–543.
[28] O. Gavet, J. Pines, Activation of cyclin B1-Cdk1 synchronizes events in the nucleus and the cytoplasm at mitosis, J. Cell Biol. 189 (2) (2010) 247–259.
[29] K. Liu, et al., *Association and clinicopathologic significance of p38MAPK-ERK-JNK-CDC25C with polyploid giant cancer cell formation*, Med Oncol 37 (1) (2019) 6.
[30] R.T. Abraham, Cell cycle checkpoint signaling through the ATM and ATR kinases, Genes Dev. 15 (17) (2001) 2177–2196.
[31] D. Hanahan, R.A. Weinberg, Hallmarks of cancer: the next generation, Cell 144 (5) (2011) 646–674.
[32] L.S. Prahl, D.J. Odde, Modeling cell migration mechanics, Adv. Exp. Med. Biol. 1092 (2018) 159–187.
[33] N.M. Aiello, et al., Upholding a role for EMT in pancreatic cancer metastasis, Nature 547 (7661) (2017) E7–E8.
[34] G. Giannelli, et al., Role of epithelial to mesenchymal transition in hepatocellular carcinoma, J. Hepatol. 65 (4) (2016) 798–808.
[35] S. Lv, et al., Inhibition of cyclinB1 suppressed the proliferation, invasion, and epithelial mesenchymal transition of hepatocellular carcinoma cells and enhanced the sensitivity to TRAIL-induced apoptosis, OncoTargets Ther. 13 (2020) 1119–1128.
[36] E.J. Sun, et al., Targeting the PI3K/Akt/mTOR pathway in hepatocellular carcinoma, Biomedicines 9 (11) (2021).
[37] S. Faes, O. Dormond, PI3K and AKT: unfaithful partners in cancer, Int. J. Mol. Sci. 16 (9) (2015) 21138–21152.
[38] S. Mabuchi, et al., mTOR is a promising therapeutic target both in cisplatin-sensitive and cisplatin-resistant clear cell carcinoma of the ovary, Clin. Cancer Res. 15 (17) (2009) 5404–5413.
[39] W. Li, et al., Activation of Akt-mTOR-p70S6K pathway in angiogenesis in hepatocellular carcinoma, Oncol. Rep. 20 (4) (2008) 713–719.
[40] Liu, Activation of Akt-mTOR-p70S6K pathway in angiogenesis in hepatocellular carcinoma, Oncol. Rep. 20 (4) (1994).
[41] F. Xu, et al., Roles of the PI3K/AKT/mTOR signalling pathways in neurodegenerative diseases and tumours, Cell Biosci. 10 (1) (2020) 54.
[42] M.S. Matter, et al., Targeting the mTOR pathway in hepatocellular carcinoma: current state and future trends, J. Hepatol. 60 (4) (2014) 855–865.
[43] J. Zhang, et al., CSTB downregulation promotes cell proliferation and migration and suppresses apoptosis in gastric cancer SGC-7901 cell line, Oncol. Res. 24 (6) (2016) 487–494.
[44] C. Chen, G. Wang, Mechanisms of hepatocellular carcinoma and challenges and opportunities for molecular targeted therapy, World J. Hepatol. 7 (15) (2015) 1964–1970.

[45] R.F. Zou, Q.H. Liu, Cloning and characterization of Litopenaeus vannamei cystainB-like in WSSV infection, Fish Shellfish Immunol. 105 (2020) 78–85.
[46] Q.S. Zhu, et al., Vimentin is a novel AKT1 target mediating motility and invasion, Oncogene 30 (4) (2011) 457–470.
[47] E. Perlson, et al., Vimentin binding to phosphorylated Erk sterically hinders enzymatic dephosphorylation of the kinase, J. Mol. Biol. 364 (5) (2006) 938–944.
[48] C. Meng, Y. Teng, X. Jiang, Raddeanin A induces apoptosis and cycle arrest in human HCT116 cells through PI3K/AKT pathway regulation in vitro and in vivo, Evid Based Complement Alternat Med 2019 (2019), 7457105.
[49] M. Zhang, et al., UBE2S promotes the development of ovarian cancer by promoting PI3K/AKT/mTOR signaling pathway to regulate cell cycle and apoptosis, Mol Med 28 (1) (2022) 62.
[50] J.C. Chambard, et al., ERK implication in cell cycle regulation, Biochim. Biophys. Acta 1773 (8) (2007) 1299–1310.
[51] M. Chen, et al., Long noncoding RNA LINC01234 promotes hepatocellular carcinoma progression through orchestrating aspartate metabolic reprogramming, Mol. Ther. 30 (6) (2022) 2354–2369.
[52] Q. Song, et al., scLM: automatic detection of consensus gene clusters across multiple single-cell datasets, Dev. Reprod. Biol. 19 (2) (2021) 330–341.